Thermophysics and Aeromechanics, *2009*, *Vol. 16*, *No. 3*

Investigation of temperature fields in supersonic flow behind a backward-facing step*

I.A. Bedarev[1], M.A. Goldfeld[1], Yu.V. Zakharova[1], and N.N. Fedorova[1,2]

[1]*Khristianovich Institute of Theoretical and Applied Mechanics SB RAS, Novosibirsk, Russia*

[2]*Novosibirsk State University of Civil Engineering, Novosibirsk, Russia*

E-mail: nfed@itam.nsc.ru

(*Received April 30, 2008*)

The results of numerical modelling and experimental investigations of high-enthalpy turbulent flows in the neighborhood of 90-degree backward-facing steps at the Mach numbers $M_\infty = 2–4$ are presented. The experiments were conducted in the hot-shot wind tunnel IT-302M of ITAM SB RAS. The computations were carried out on the basis of the full Favres-averaged Navier — Stokes equations augmented by the Wilcox turbulence model. The temperature factor influence on the flow structure in the separated zone and temperature distributions was investigated numerically for different Mach numbers. The wall temperature is shown to affect significantly the quantity and sizes of recirculation vortices as well as the temperature distribution in the zone of flow separation and reattachment. The computational results are compared with experimental data on the pressure distribution on the model surface and the wave structure of the flow.

Key words: high-enthalpy flows, separation, mathematical modelling, turbulence.

INTRODUCTION

The scramjet is the key element of promising high-velocity flying vehicles. The efficiency of the engine and of the entire flying vehicle is affected substantially by the fuel ignition processes in combustor. The hypersonic ($M > 5$) flow of air decelerates at its passage through the inlet and isolator and, as a rule, has moderately supersonic velocities ($M = 2–3$) at the combustor inlet. At such flow velocities, the typical times of the mixture stay in combustor are small, and, hence, the gas must have a fairly high temperature for ignition and stable combustion in fuel supply regions.

A diverging duct (the duct with a backward-facing step/cavity) is a conventional geometric configuration for the arrangement of subsonic recirculation zones used for combustion stabilization in supersonic flow [1]. It is assumed that the necessary static temperature of the flow in the ignition zone can be ensured by high values of the total temperature $T_0 > 1500$ K. As the investigations, however, show, the temperature fields of

* The work was financially supported by the Russian Foundation for Basic Research (Grants Nos. 07-08-00420 and 09-08-01001-a), AVTsP "Development of scientific potential of higher school (2009-2010)" for the year 2009 (project code 2.1.1/4674).

high-enthalpy flows in the neighborhood of the duct expansion are very nonuniform. Expansion waves, cold duct walls, the cold fuel injection or thermal protection of the walls with the aid of cold jets may lead to the formation of local relatively cold and hot zones in the flow. The ignition efficiency depends on how the fuel supply is arranged.

During the last decades, numerous analytic, numerical, and experimental investigations of supersonic flows behind the backward-facing steps [1–6] were carried out. Detailed studies of the wall temperature influence on the parameters of separated flows near the compression corner [4], behind the cylinder and sphere are also known [7]. At the same time, the data on the temperature factor influence on the parameters of flows behind a backward-facing step are very limited. These results are of especial importance at the investigations of high-enthalpy flows in the facilities of short-time operation for which the relative wall temperature variation in a wide range during one experiment is typical. The flows near forward-facing steps were studied in [8, 9] for the conditions of the cold (T_0 = 300 K) and high-enthalpy (T_0 = 2500 K) external flow at M_∞ = 3 and 4. It was shown that the temperature conditions may affect significantly the temperature distribution and flow structure behind the backward-facing step. It was shown, in particular, that the vortex structure of the separated zone depends on the temperature factor. The present paper presents some results of the works [8, 9], for example, for M_∞ = 4. Previous studies were limited to the region of moderately cold values of the wall temperature. The present work continues the investigation of the temperature factor influence in a wide range as well as for other Mach numbers and flow parameters.

The study of the structure of planar supersonic turbulent flows behind the backward-facing step at different Mach numbers M_∞ = 2–4 is the main purpose of the present work. The problem is investigated by the mathematical modelling methods based on the Favres-averaged Navier — Stokes equations augmented by the Wilcox k–ω model of turbulence. The computations were carried out for the conditions of the wind tunnel IT-302M of ITAM SB RAS. The flow patterns are obtained for several values of the temperature factor, and the pressure and skin-friction distributions are determined along the model surface. The profiles in different sections are also obtained. The flow patterns are compared with the experimental shadow photographs. The computed and experimental data on the static pressure distribution along the wall are compared.

CONDITIONS OF EXPERIMENTS

Experimental investigations were carried out in the hot-shot setup IT-302M of ITAM SB RAS [10], which enables the investigations in the attached pipeline regime in a wide range of the Mach numbers M = 2–12 at the maximum total pressure P_0 = 40 MPa, total temperature T_0 = 2500 K, and the duration of the regime up to 200 ms. The exchangeable profiled nozzles enable the obtaining at the duct inlet of a flow with the Mach numbers from 2 to 5 [11]. The experimental model (Fig. 1) represents a duct consisting of an interval of constant cross section of the width d = 50 mm, length L = 300 mm, and the diverging part. A backward-facing step of height h lies on the upper wall. At the execution of experiments, a Pitot pressure rake was installed to control the supersonic flow uniformity in the constant section of isolator. The strain gage transducers of static pressure with the nominal values of 1.6, 4, and 10 bars were mounted along the model length. The executed assessment of the accuracy of measurements in the hot-shot wind tunnel showed that the pressure was measured with the root-mean-square error of 1–1.5 %. A shadow visualization of the flow was also carried out in experiment. To obtain the shadow photographs of the flows the device IAB-451 was used with a constant source of light. The rapid measuring system operated in its coordination with

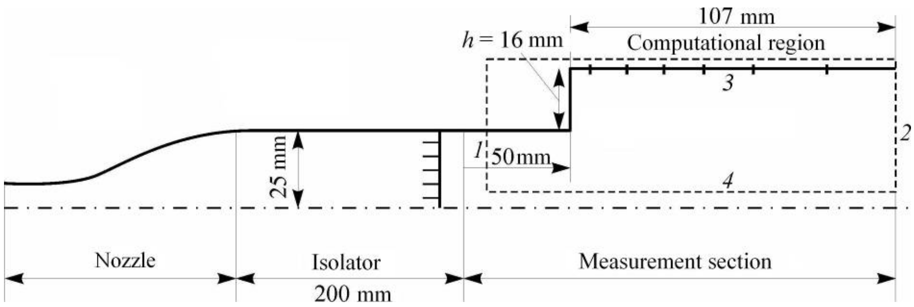

Fig. 1. Experimental model schematic and computational region.

the aerophysical multi-user experimental database "ARROW" [12] for the information acquisition, processing, and representation.

Table 1 presents the parameters of the flows investigated in the present paper. Here M_∞ is the Mach number ahead of the backward-facing step, P_0 and T_0 are the pressure and stagnation temperature, h is the backward-facing step height, and Re_h is the Reynolds number computed from the reference size h, P_∞ and T_∞ are the freestream static pressure and temperature, $T_{w.\ ad}$ is the wall adiabatic temperature for the given conditions.

MATHEMATICAL MODEL, BOUNDARY CONDITIONS, NUMERICAL METHOD, AND THE GRID

The computations of planar flows for the parameters indicated in Table 1 were carried out with the aid of the in-house code for solving the full unsteady Favres-averaged Navier — Stokes equations augmented by the Wilcox two-parameter turbulence model with a correction for the compressibility effect [13]. An implicit first-order scheme was used for the temporal approximation of equations, which was implemented with the aid of the fractional-step method [14]. The steady solutions were computed by the steadying method. The numerical solution was assumed steady upon reaching the condition $\max\limits_{i,j}\left(\partial\rho/\partial t\right)_{ij} < 10^{-2}$. Spatial derivatives were approximated by using the "conservation law" form of the equations, which ensured the satisfaction of conservation laws in the problems under study. Convective terms of the equation were approximated with the aid of a third-order TVD scheme, and the viscous terms were approximated by the second-order central finite differences.

The above program package was previously used successfully for the computations of supersonic turbulent separated flows in the neighborhood of the steps/backward-facing steps with different angles of the windward/leeward face [15], an oblique shock impinging onto the plate [16], the inlets [17], and other configurations [18, 19].

The computational region of the problem shown in Fig. 1 by the dashed line includes only part of the physical model, which directly adheres to the backward-facing step, rather

Table 1

Parameters of investigated flows

M_∞	h, mm	$P_0 \times 10^6$, Pa	T_0, K	$Re_h \times 10^5$	$P_\infty \times 10^6$, Pa	T_∞, K	$T_{w\ ad}$, K
2.0	16	1.5	1200	5.1	0.192	667	1141
2.33	16	1.8	1400	4.1	0.138	690	1361
2.8	16	3.0	2000	7.6	1.55	778.8	1963
3.5	25	13.0	3000	9.4	0.172	869	2766
4.0	25	30	2500	19.3	0.197	595.2	2290

than the entire model, and is bounded by the inlet (1) and outlet (2) sections on the left and on the right, by the model surface (3) at the top, and by the free surface (4) at the bottom.

The computations of the flow were carried out within the framework of the boundary layer model from the nozzle critical section and the entire isolator section to obtain the profiles of gasdynamic and turbulent parameters in the inlet section (1) for different values of the temperature factor. The pressure gradient in the nozzle diverging part was obtained from the quasi-one-dimensional gasdynamic theory under the assumption of the gas flow rate equality. The computations within the framework of the boundary layer with an external pressure gradient showed that under the given conditions, the inlet section of the computational region lies in the region of a developed turbulent boundary layer. Since the measurement of profiles is impossible under the conditions of the hotshot wind tunnel, the comparisons with experiments were conducted in terms of the Mach number, which is affected by the boundary-layer thickness on the duct walls.

The "soft" conditions of extrapolation were set in the outlet section (2). Since a bounded region in the neighborhood of the backward-facing step was the research subject, the influence of the model lower wall was not considered. The lower boundary (4) of the computational region was assumed free, and the non-reflecting conditions of the simple wave type were set on it. The no-slip conditions for the velocity were used on the model surface (3), and the conditions for temperature on this surface were of two kinds: the adiabatic temperature conditions $\partial T/\partial n|_{\text{wall}} = 0$ or the conditions of the temperature constancy $T|_{\text{wall}} = T_{\text{w}}$. The T_{w} value was varied in the range from 300 K to the values corresponding to the adiabatic wall condition. The temperature factor value K_T was computed as the ratio of the wall temperature T_{w} to the total temperature T_0 for the given Mach number. The computational region was turned for convenience in the vertical direction by 180°.

A regular rectangular grid with a clustering of nodes in the direction of solid surfaces was generated in the computational region. In most computations, the grid contained 200–300 nodes in the y direction and 300–500 nodes in the x direction. The minimum size of the difference grid step near the model surface was chosen in such a way that $y_1^+ \sim 1$ for the chosen freestream conditions. About five computational nodes got into the laminar sublayer $y^+ < 12$, which ensured its sufficient resolution. The grid step stretching parameter at the motion from the surface did not exceed 1.1, which also agreed with the recommendations accepted in the literature and our experience in computation of turbulent separated flows [14–19].

Because of high temperature and, consequently, density gradients the minimum steps along the normal to the surfaces were of the order of 10^{-5} (in dimensionless variables), which resulted in a very severe condition on the time step. Under these conditions, a further grid refinement became technically impossible, and the grid "worsening" was used for convergence investigation, that is the grid was restructured inside the boundary layer by increasing y_1^+ up to the value of 10 and altering the clustering law near the surface. This resulted in no changes in the pressure distributions as well as in the fields of gasdynamic parameters, and the coefficients of the skin friction and heat fluxes changed by no more than 10 %, which confirmed the convergence on the grid.

COMPUTATIONAL RESULTS

In computations at Mach number $\text{M}_\infty = 2$, the adiabatic temperature conditions and the cold wall conditions were used, which are presented in Table 2 together with the integral thicknesses of the turbulent boundary layer as well as the base pressure values P_b obtained in computations.

Table 2

Parameters of computations

M_∞	T_w, K	δ, $\times 10^{-3}$ mm	δ^* $\times 10^{-4}$ mm	P_b/P_∞	δ/h
2.0	300	5.1	6.1	0.45	0.32
	500	4.9	7.3	0.37	0.30
	900	4.7	8.3	0.34	0.29
	adiabat.	4.2	9.7	0.33	0.26
2.33	300	5.6	8.3	0.26	0.35
2.8	300	5.9	11.6	0.16	0.37
3.5	300	9.02	4.9	0.35	0.36
	700	8.54	4.6	0.20	0.34
	1500	7.96	11.3	0.22	0.32
	adiabat.	7.34	9.3	0.25	0.29

Figure 2 shows the static pressure and the skin-friction coefficient distributions along the model surface. The point $x/h = 0$ corresponds to the external, and $x/h = 1$ to the internal angle of the configuration. The pressure and the skin friction were nondimensionalized by the corresponding values ahead of the backward-facing step. For a cold temperature of the wall at $T_w = 300$ K (see Fig. 2, *a*, curve *1*) in the base region, the observed pressure level was by the factor of 1.5 higher in comparison with the adiabatic conditions and higher T_w. When increasing T_w from 300 to 500 K the pressure level in the base region drops, and the pressure recovery occurs faster, which is related to a reduction of the separated zone sizes (see Fig. 2, *a*). The skin-friction coefficient distribution confirms the variation of separated zone sizes at the wall temperature increase (see Fig. 2, *b*). A nonmonotonous behavior of the skin-friction coefficient inside the separated zone at $1 < x/h < 3$ and the appearance of extra points with a zero surface friction points to the presence of the secondary flow separation at the reverse flow motion from the divergence point to the configuration internal corner. A flow overexpansion is observed near the external corner of the backward-facing step, which can be identified by a peak (the local minimum) in the pressure distribution. The existence of a lip shock, which was fixed in computations, is related to this peculiarity of the flow. The lip shock strength was insignificant at the considered flow parameters, and the shock did not affect significantly the flows in the investigated zone.

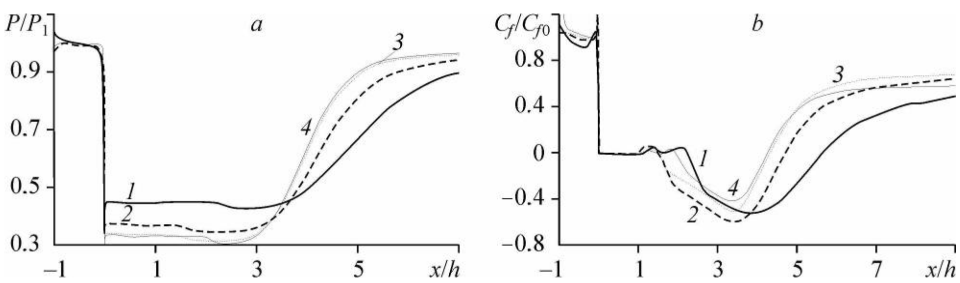

Fig. 2. Distributions of the pressure (*a*) and surface friction (*b*) along the model surface at $M_\infty = 2$. $T_w = 300$ (*1*), 500 (*2*), 900 (*3*) K, the adiabatic wall (*4*).

A local maximum related to a restructuring of the flow profiles is also observed on the skin-friction distribution near the external corner. The existence of the above peak in the skin-friction distribution agrees with the analytic investigations of [6]. The value of the skin-friction coefficient along the vertical leeward face of the backward-facing step is by two orders of magnitude lower than in other regions, which is due to low values of the velocity gradients in the direction along a normal to the wall. This leads to that the values of the skin-friction coefficient are close to zero on the graphs, which does not enable the identification of the internal structure of the separated zone.

To analyse the influence of the temperature factor K_T on the vortex structure of the flow in the recirculation zone the temperature fields and the streamlines were plotted (Fig. 3). The wall temperature T_w variation affects significantly the flow vortex structure and the temperature fields. A high temperature was obtained for all considered values of the temperature factor in the region of flow reattachment, and the temperature of the mixing layer is close to the external flow temperature. A clockwise rotating vortex, which transfers a hot gas inside the separated zone, adheres to the mixing layer. Near the butt end of the backward-facing step, there exists a vortex of the opposite direction the size of which changes at the wall temperature reduction. Under the adiabatic conditions, the vortices have about the same sizes, and the third clockwise vortex is observed in the internal corner of the configuration (see Fig. 3, *a*). At a wall temperature drop, the external vortex size grows, and the butt-end vortex size decreases, and the internal vortex disappears (see Fig. 3, *b*, *c*). A further drop of the wall temperature down to $T_w = 300$ K leads to the fact that the three-vortex structure is restored (see Fig. 3, *d*). The gas temperature in the separated zone is much lower than that under the adiabatic temperature conditions. The expansion waves whose source is a low pressure at the external vortex center propagate from the separated zone to the external flow (see Fig. 3, *d*). This

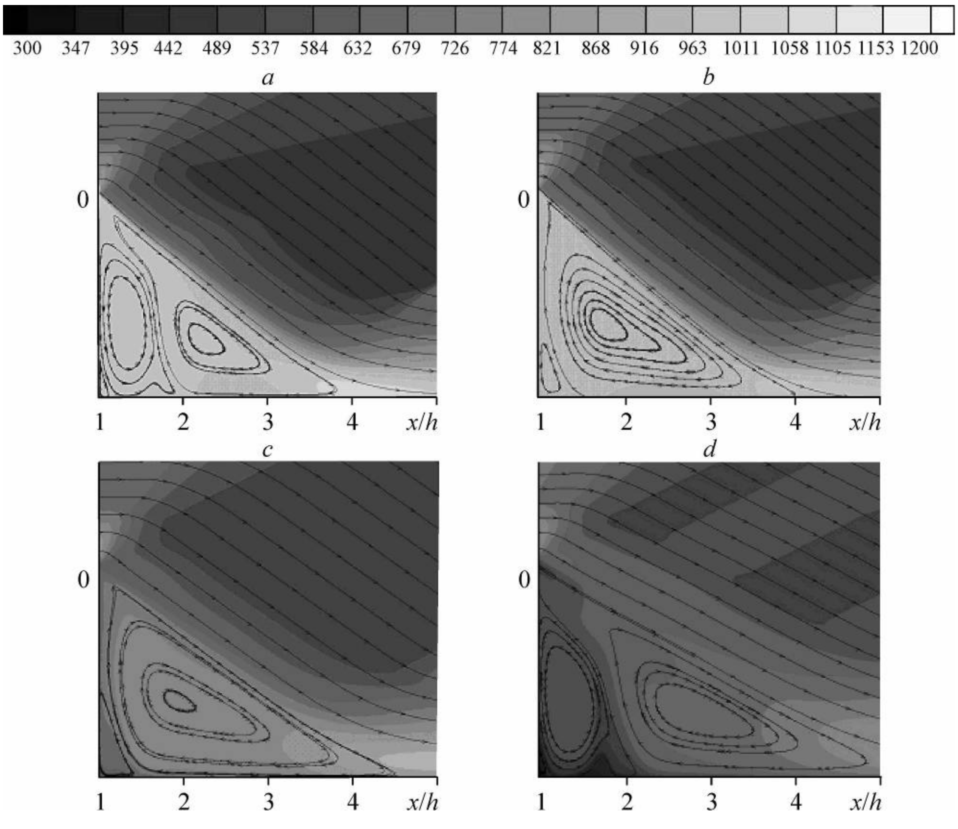

Fig. 3. Temperature fields and streamlines at $M_\infty = 2$ for the conditions of the adiabatic (*a*) and cold (*b*, *d*) walls at $T_w = 900$ (*b*), 500 (*c*), 300 (*d*) K.

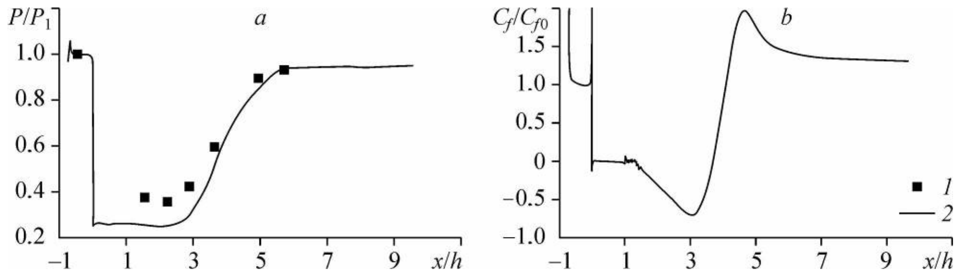

Fig. 4. Distributions of the pressure (*a*) and skin friction (*b*) along the surface at $M_\infty = 2.33$ for $T_w = 300$ K.

1 — experiment, *2* — computation.

pressure drop manifests itself in the pressure distribution (see Fig. 2, *a*) in the range $2.5 > x/h > 3.5$.

At $M_\infty = 2.33$, the numerical investigations were carried out for the conditions of experiments in the IT-302M (row 2, see Table 1). Figure 4 shows the static pressure and surface friction distributions for the cold wall conditions (T_w = 300 K). Symbols show experimental data. A comparison of numerical results with experimental data on the pressure distribution on the wall (see Fig. 4, *a*) shows that the computation predicts correctly the separated zone length. A discrepancy of numerical and experimental data in the base pressure level may be attributed to a possible discrepancy in numerical and experimental parameters of the boundary layer ahead of the backward-facing step. As was noted above, no profiles were measured ahead of the backward-facing step. The profiles of all parameters in the inlet section were computed from the boundary layer model.

At the Mach number $M_\infty = 2.8$, the computations were carried out for the conditions presented in Table 1. A comparison of the computed and experimental data on the pressure distribution on the cold wall (T_w = 300 K), which is illustrated in Fig. 5. *a*, shows their good agreement in the base region and downstream from the reattachment point. The separated zone length obtained in computation agrees well with experimental results (see Fig. 5, *b*). The density gradients obtained in computation (*a*) and the experimental shadow flow pattern (*b*) are compared in Fig. 6 for the case $M_\infty = 2.8$, T_w = 300 K. The comparison shows that the computation reproduces correctly the slopes of the first and last characteristics of the expansion wave fan (EF) as well as the recirculation zone (RZ) length and the tail shock (TS) location.

The computed results are further presented for the Mach number $M_\infty = 3.5$ and the total temperature T_0 = 3000 K. Figure 7 shows the distributions of the pressure and skin friction for a few values of T_w. One should note a considerable increase in the separated

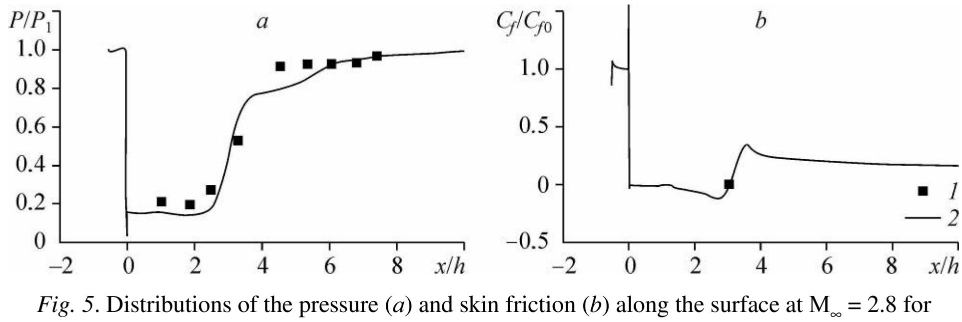

Fig. 5. Distributions of the pressure (*a*) and skin friction (*b*) along the surface at $M_\infty = 2.8$ for T_w = 300 K.

1 — experiment, *2* — computation.

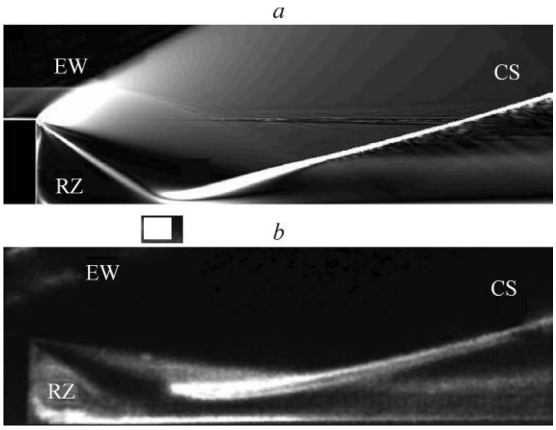

Fig. 6. Computed density field (*a*) and the experimental flow pattern (*b*) for $M_\infty = 2.8$.

zone length for the case $T_w = 300$ K (see Fig. 7, *b*, curve *1*). This appears to be related to a low value of the temperature factor and a large jump between the adiabatic (T_{ad} = 2800 K) and static (T_{st} = = 870 K) temperatures. An increase in the wall temperature up to 700 K (curve *2*) leads to an abrupt shortening of the separated region. However, at T_w = 1500 K and under the adiabatic conditions (curves *3* and *4*), the separated zone length increases.

Under the adiabatic and moderately cold temperature conditions, the pressure growth behind the reattachment point occurs nonuniformly. The possible reasons for such a nonuniformity of the pressure behavior at the flow over the backward-facing steps were discussed in [18]. It was shown in this work that the secondary compression waves moving towards the wall arise at the tail shock passage through the mixing layer. Right this gives rise to the second region with a higher pressure gradient. The static pressure field for the case M_∞ = 3.5 and T_w = 700 K is presented in Fig. 8, which shows 50 contours in the range $2\cdot10^4$–$2\cdot10^5$ Pa. One can see in the figure the expansion fan, the tail shock, and the above-described secondary compression waves, which come to the lower surface of the backward-facing step at $6 < x/h < 7$ and further reflect from it and catch up the tail shock.

Figure 9 shows the static pressure distribution at $M_\infty = 4$ for different temperature factors. Curve *1* corresponds to the cold flow conditions (T_0 = 500 K) under the adiabatic conditions on the wall, curves *2*, *3*, and *4* are the numerical results obtained for the conditions of a high-enthalpy setup under the adiabatic (curve *2*) and cold (curve *3* at T_w = 1832 K, curve *4* at T_w = 1145 K) conditions on the wall. It is seen in the figure that at a reduction of the wall temperature down to moderately cold values (T_w = 1145 K) one observes a reduction of the separated zone length and an insignificant drop of the base pressure. No computations were carried out in this case for lower wall temperatures.

For a quantitative estimation of the variation of flow parameters depending on the value of the temperature factor K_T at M_∞ = 3.5, the profiles were plotted in three cross sections S1–S3 located ahead of the backward-facing step, in the recirculation zone, and near the flow reattachment point (see Fig. 8).

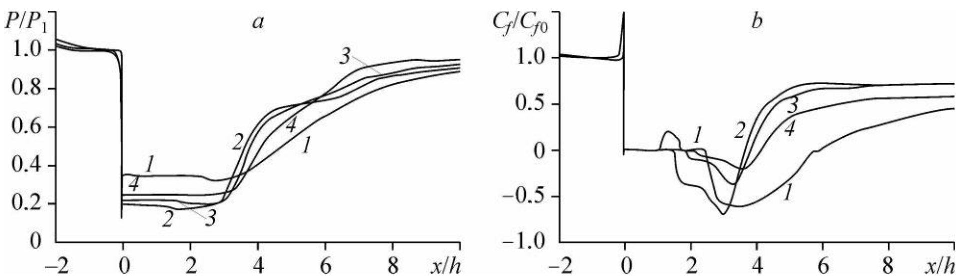

Fig. 7. Distribution of the pressure (*a*) and skin friction (*b*) for M_∞ = 3.5.
T_w = 300 (*1*), 700 (*2*), 1500 (*3*) K, the adiabatic wall (*4*)

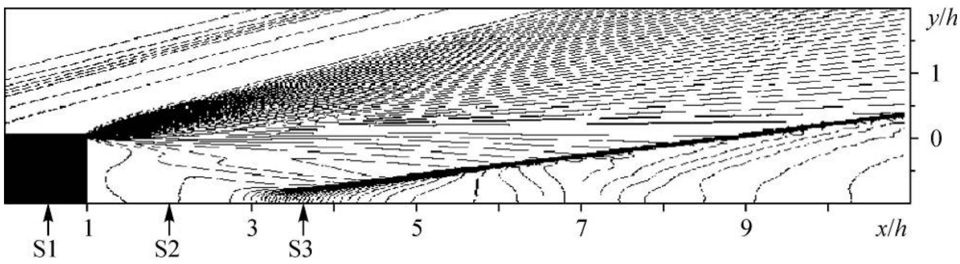

Fig. 8. Static pressure contours for $M_\infty = 3.5$ at $T_w = 700$.

Fig. 9. Pressure distributions for $M_\infty = 4$.
1 — "cold flow" under the adiabatic conditions on the wall, *2* — the "hot flow" with the adiabatic wall, *3* — the "hot flow; T_w = 1832 (*3*), 1145 (*4*) K.

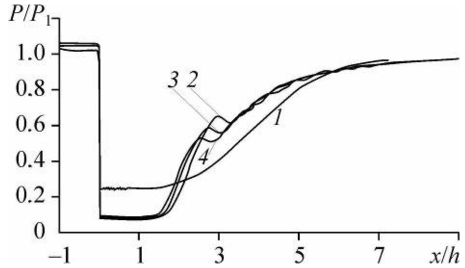

Figures 10–12 show the profiles of the temperature, density, velocity, and turbulent kinetic energy (TKE). Digits *1–4* mark in the figures the numerical results obtained at T_w = 300, 700, and 1500 K and under the adiabatic conditions, respectively.

In section S1 lying ahead of the interaction zone, the variation of the temperature factor K_T leads to a substantial alteration of the profiles of all parameters (see Fig. 10). Under the adiabatic conditions, the flow has a high temperature gradient near the surface, which gives rise to high density gradients. At a wall temperature reduction down to the value T_w = 1500 K, the profiles of the temperature and, consequently, density near the surface are nonmonotonous. The temperature has a local minimum on the wall, then it grows in a fairly narrow zone near the surface because of the viscous dissipation effect, which results in the local maximum formation. The temperature further drops monotonously to the freestream temperature T_∞ = 711 K (see Fig. 10, *a*). The temperature

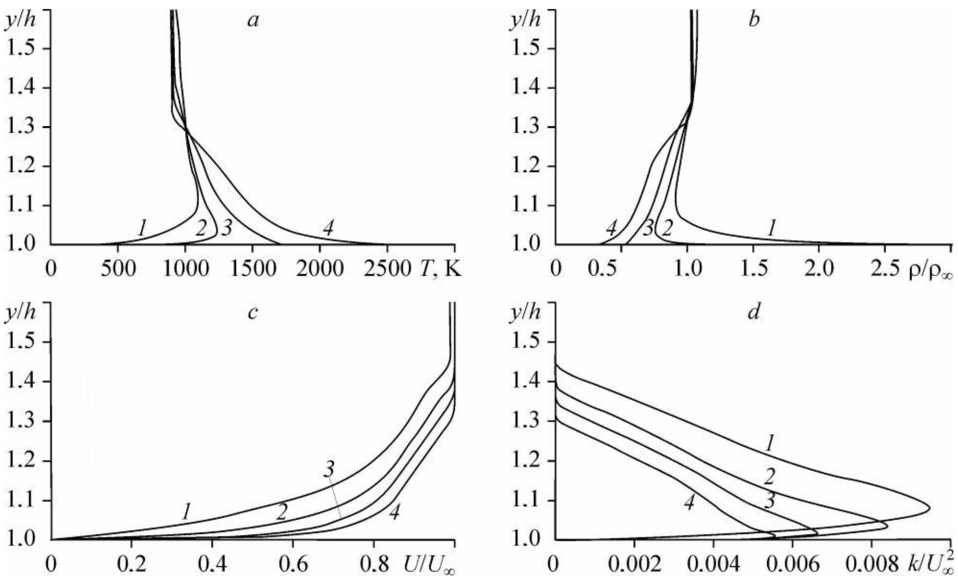

Fig. 10. Profiles of the temperature (*a*), density (*b*), velocity (*c*), and TKE (*d*) for $M_\infty = 3.5$ in section S1.

T_w = 300 (*1*), 700 (*2*), 1500 (*3*) K, the adiabatic wall (*4*).

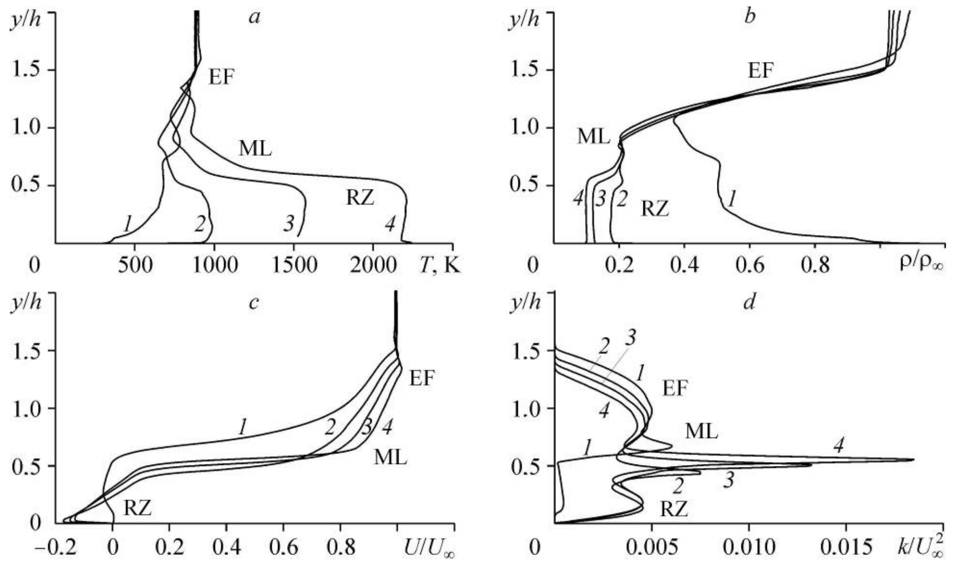

Fig. 11. Profiles of the temperature (*a*), density (*b*), velocity (*c*), and TKE (*d*) for $M_\infty = 3.5$ in section S2.

T_w = 300 (*1*), 700 (*2*), 1500 (*3*) K, the adiabatic wall (*4*).

and density profiles are more uniform at a moderately cold temperature of the wall T_w = 700 K, which is close to the freestream temperature. However, by virtue of the viscous dissipation near the wall, the temperature profile remains nonmonotonous. Under the conditions of the coldest wall T_w = 300 K, the static temperature of the flow grows up to 1080 K, and then it drops down to T_∞.

The next section S2 lies in the middle part of the separated zone, which is evidenced by the negative values on the mean velocity profiles (see Fig. 11, *c*). The graphs show a weak influence of the temperature factor on the mean velocity profiles in

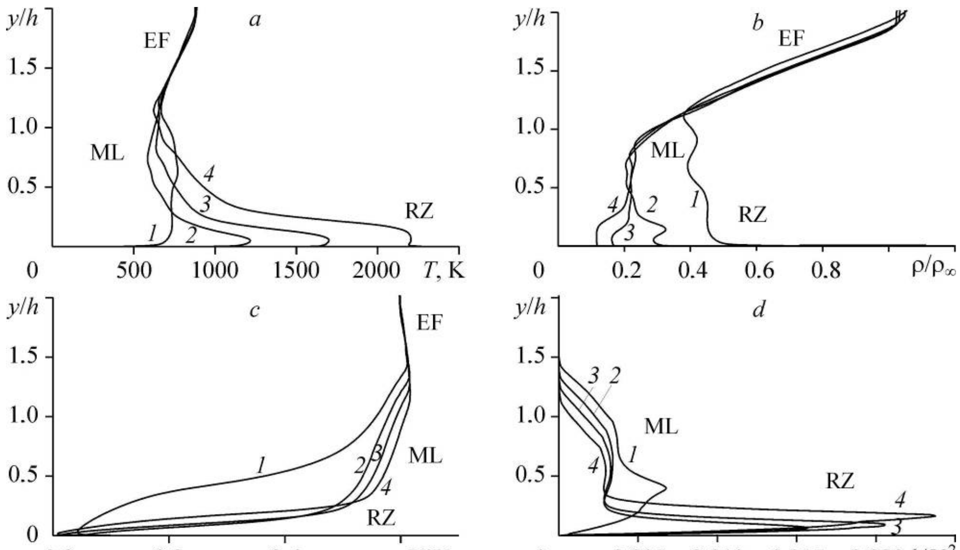

Fig. 12. Profiles of the temperature (*a*), density (*b*), velocity (*c*), and TKE (*d*) for $M_\infty = 3.5$ in section S3.

T_w = 300 (*1*), 700 (*2*), 1500 (*3*) K, the adiabatic wall (*4*).

the mixing layer (ML) located at 0.5 > y/h > 0.9. Note that for T_w = 300 K, the mixing layer lies higher than for other values of T_w. The expansion fan (EF), which is passed by the section x = const in the "reverse" direction, that is from the region of a lower pressure to the region of a higher pressure, lies above the mixing layer. One observes inside the recirculation zone (RZ) a significant difference in the temperature and density profiles, and for T_w = 300, the density near the wall is close to the freestream density (see Fig. 11, *b*). The temperature and density profiles for different T_w differ significantly in the separated zone and in the mixing layer. The TKE graphs (see Fig. 11, *d*) have three local maximums, the first of which lies in the reverse flow region, and the second lies in the inflection line in the mean velocity profiles, and the third lies in the central part of the mixing layer.

Section S3 lies near the reattachment point in the zone of compression waves. The expansion wave approaches closer the body surface — 2.0 > y/h > 1.1, the recirculation zone is fairly narrow — 0.3 > y/h > 0, and in the case of T_w = 300 K, the transverse size of the recirculation zone is much larger than for other values of T_w (see Fig. 12, *c*). For the adiabatic and moderately cold values of T_w on the boundary of the mixing layer and the recirculation zone, high temperature gradients exist, and in the case of T_w = 300 K, the temperature distribution is more uniform (see Fig. 12, *a*). One sees in the TKE graphs two local maximums, the lower one, more appreciable, corresponds to the inflection line of the velocities, and the upper one corresponds to the mixing layer.

CONCLUSIONS

The numerical investigations of the temperature factor influence on the structure of supersonic high-enthalpy turbulent flows in the neighborhood of the backward-facing steps were carried out at M_∞ = 2–4 and at the wall temperature variation from the adiabatic values up to T_w = 300 K. The temperature conditions on the wall were shown to affect all the flow parameters in the interaction zone. At a reduction of the wall temperature T_w the separated zone size and the base pressure vary nonmonotonously.

A comparison of computational results with experimental data on the pressure distribution on the wall, the flow structure and the separated zone length showed a satisfactory agreement. The estimation of vortex structure, the fields of temperature and pressures in the recirculation zone may be used at the execution of experimental investigations of the ignition and combustion processes in short-duration wind tunnels for choosing the location of fuel supply to the zone with an optimal temperature level for fuel ignition.

REFERENCES

1. **K. Uenishi, R.C. Rogers, and G.B. Northam,** Numerical predictions of a rearward-facing-step flow in a supersonic combustor, J. Propulsion, 1989, Vol. 5, No. 2, P. 158−164.
2. **L.V. Gogish and G.Yu. Stepanov,** Turbulent Separated Flows, Nauka, Moscow, 1979.
3. **D.R. Chapman,** An analysis of the base pressure at supersonic velocities and comparison with experiment, 1951 — NACA TR No. 1051.
4. **N.F. Krasnov, V.N. Koshevoy, and V.T. Kalugin,** Aerodynamics of Separated Flows, Vysshaya shkola, Moscow, 1988.
5. **A.P. Shvets and I.T. Shvets,** Near-Wake Gas Dynamics, Nauk. dumka, Kiev, 1976.
6. **V.Ya. Neyland, V.V. Bogolepov, G.N. Dudin, and I.I. Lipatov,** Asymptotic Theory of Supersonic Flows of Viscous Gas, Fizmatlit, Moscow, 2004.
7. **V.A. Bashkin, I.V. Egorov, M.V. Egorova, and D.V. Ivanov,** Supersonic laminar-turbulent gas flow past a circular cylinder, Fluid Dyn., 2000, Vol. 35, No. 5, P. 652−662.
8. **I.A. Bedarev, N.N. Fedorova, and M.A. Goldfeld,** Turbulent flows over backward facing steps, in: Proc. Fifth Europ. Symp. on Aerothermodyn. for Space Vehicles, ESA SP-563, February, 2005, P. 311–316.
9. **N.N. Fedorova and I.A. Bedarev,** Numerical simulation of supersonic turbulent flows over backward facing steps, in: Computational Fluid Dyn. 2006, in: Proc. Fourth Int. Conf. on Computational Fluid Dynamics, ICCFD 4, Ghent, July 10–14, 2006, Springer-Verlag, Berlin et al., 2009, P. 713−718.

10. **L.N. Puzyrev and M.I. Yaroslavtsev,** Stabilization of gas parameters in the settling chamber of a hypersonic hot-shot wind tunnel, Izv. SO AN SSSR. Ser. tekhn. nauk, 1990, Iss. 5, P. 135–140.
11. **M.A. Goldfeld, A.V. Starov, V.A. Vinogradov et al.,** Methodical aspects of the study of supersonic combustor in the impulse regime, in: Proc. Int. Conf. on the Methods of Aerophys. Research, Vol. 1, Novosibirsk, 1996, P.123–129.
12. **Yu.V. Semenova and R.V. Nestoulia,** Database technologies for aerodynamic experiment results storage, processing, analysis and presentation, in: Proc. Int. Conf. on the Methods of Aerophys. Research. Pt. II, Publ. House "Nonparel", Novosibirsk, 2004, P. 147–152.
13. **D.C. Wilcox,** Turbulence modelling for CFD, DCW Ind. Inc., La Canada, California, 1993.
14. **A.V. Borisov and N.N. Fedorova,** Computation of turbulent separated flows based on a method of higher approximation order, Thermophysics and Aeromechanics, 1995, Vol. 2, No. 3, P. 253–269.
15. **I.A. Bedarev, A.V. Borisov, and N.N. Fedorova,** Numerical simulation of the supersonic turbulent separated flows in vicinity of the backward and forward faced steps, Comp. Fluid Dyn. J., 2001, Vol. 10. Spec. Number, P. 194–202.
16. **N.N. Fedorova, I.A. Fedorchenko, and E.E. Shuelein,** Experimental and numerical study of oblique shock wave / Turbulent boundary layer interaction at M = 5, Comp. Fluid Dyn. J., 2001, Vol. 10, No. 3. P. 376–381.
17. **I.A. Bedarev, N.N. Fedorova, M.A. Goldfeld, and F. Falempin,** Mathematical modelling of supersonic turbulent flows in inlets with rotating cowl, in: Comput. Fluid Dyn. 2004 (Proc. ICCFD-3), Springer-Verlag, 2006, Berlin et al., P. 295–300.
18. **I.A. Bedarev and N.N. Fedorova,** Structure of supersonic turbulent flows in the neighborhood of backward-facing steps, J. Appl. Mech. Tech. Phys., 2006, Vol. 47, No. 6, P. 48–58.
19. **I.A. Bedarev, A.A. Maslov, A.A. Sidorenko. N.N. Fedorova, and A.N. Shiplyuk,** Experimental and numerical investigation of the hypersonic separated flow in the neighborhood of a cone with a skirt, J. Appl. Mech. Tech. Phys., 2002, Vol. 43, No. 8, P. 100–112.